IJIE

http://penerbit.uthm.edu.my/ojs/index.php/ijie

The International Journal of Integrated Engineering

ISSN : 2229-838X e-ISSN : 2600-7916

Multi-Phase Nano Fluid Natural Convection in A Partially Divided Cavity for Cooling of Radioactive Waste Containers

Mohammad Mohsen Peiravi[1], Javad Alinejad[2*], Davood Domiri Ganji[3]

[1]Department of Mechanical Engineering,
Technical and Vocational University (TVU), Tehran, IRAN

[2]Department of Mechanical Engineering,
Sari branch, Islamic Azad University, Sari, IRAN

[3]Department of Mechanical Engineering,
Babol Noshirvani University of Technology, Babol, IRAN

DOI: https://doi.org/ 10.30880/ijie.2022.14.06.001
Received 20 August 2020; Accepted 29 May 2021; Available online 10 November 2022

Abstract: The innovation of this investigation is fins arrangement effects on Al2O3-water Nano fluid natural convection in a partially divided cavity for energy storage systems and cooling of radioactive waste containers. Simulation of fluid velocity and temperature fields done based on the Lattice Boltzmann Model using the D2Q9 and D2Q5 methods, respectively. Streamline, isotherm, Nusselt number, velocity and temperature fields have been studied for different shapes of fins. In this investigation, we surveyed 4 shape of fins that arranged in three cases; case 1: yL=0.25 L, yR=0.75 L, case 2: yL=0.5 L, yR=0.5 L and Case 3: yL=0.75 L, yR=0.25 L. The results illustrated, assuming case 2: yL=0.5 L, yR=0.5 L is base case, so with changing arrangement of fins for case 1: yL=0.25 L, yR=0.75 L, rate percentage of average Nusselt number for cavities arranged with rectangular, circle, vertical and horizontal Ellipse fins were %26, %8, %4 and %8, respectively. Furthermore, with changing arrangement of fins to case 3: yL=0.75 L, yR=0.25 L, these percentages were %62, %24, %14 and %22.

Keywords: Fins shape effects, fins arrangement effects, lattice Boltzmann method, multi-phase Nano fluid, natural convection, partially divided cavity

1. Introduction

Multi-phase Al_2O_3-water Nano fluid natural convection with fins arrangement effects in a partially divided cavity practically investigated for energy storage systems and cooling of radioactive waste containers. So, experimentally, numerically or analytically results represented as follows.

researchers performed the investigation with periodic boundary conditions in the direction of developed flow with the production of hydrodynamic and heat source [1, 2]. Scholars Investigated the hybrid natural convection heat transfer between saturated fluid in porous media with thermal surfaces [3, 4]. researchers solved internal flow problem involving fluid-solid hybrid natural convection heat transfer with new compressible particle hydrodynamics method [5, 6]. Scientists modeled hybrid natural convection heat transfer on steam Reforming of Ethanol (SRE) to produce hydrogen in a micro-channel system [7, 8]. Scholars simulated coupled hybrid natural convection heat transfer and heat generation in open-cell ceramic foams used in a turbulent system with constant temperature of surface [9, 10]. researchers analyzed the high-temperature behavior in a double-pipe heat exchanger filled with open-cell porous foam [11, 12]. Scientists analyzed in-tube thermodynamic development on incomplete and complete condensation inside finned tube condensers [13, 14]. researchers investigated experimentally and numerically, hybrid natural convection heat transfer and overall

*Corresponding author: Alinejad_javad@yahoo.com

cooling effectiveness of a vane end surface for a high-pressure turbine [15, 16]. Scientists modeled hybrid natural convection heat transfer characteristics of the cryo-supersonic air-quenching on collocated curvilinear grids [17]. Recently, authors numerically and experimentally simulated hybrid natural convection Nano fluid through a horizontal microchannel and fluid flow transitions of a heating element on the enclosure [18].

In the present study, a combination of Al2O3-water Nano fluid natural convection with fins arrangement effects in a partially divided cavity practically surveyed for energy storage systems and cooling of radioactive waste containers. The fluid velocity and temperature fields on the rectangular, Circle, vertical and horizontal Ellipse fins simulated based on the Lattice Boltzmann Model using the D2Q9 and D2Q5 methods, respectively in Matlab software.

Nomenclature	
k_b	Boltzmann constant
C_i	lattice velocity
C_s	speed of sound
x, y	coordinates (m)
L	dimensions of cavity (m)
f_i	particle density distribution function
f_i^{eq}	equilibrium particle density distribution function
g_i	particle energy distribution function
g_i^{eq}	equilibrium particle energy distribution function
g_y	gravitational acceleration (m/s^2)
n_1, n_2	relaxation time constants
Nu_m	mean Nusselt number
Nu_y	local Nusselt number (h.x/k)
d_s	spherical particle diameter of the solid (m)
d_f	spherical particle diameter of the fluid (m)
d_{nf}	nanofluid spherical particle diameter (m)
ω_i	lattice grade weight
T_c	temperature of the cold wall (K)
T_h	temperature of the hot wall (K)
α_{nf}	nanofluid thermal diffusivity of the fluid (m2/s)
β_{nf}	nanofluid thermal expansion (1/K)
ρ_{nf}	nanofluid density (kg/m3)
μ_{nf}	nanofluid dynamic viscosity (kg/m. s)

2. Problem Definition

In this paper, the multi-phase Al2O3-water Nano fluid natural convection heat transfer in a partially divided cavity with arrangement of different shape of fins is presented. The flow and heat transfer characteristics are optimized with arrangement rectangular, Circle, vertical and horizontal Ellipse fins. The boundary conditions for the mentioned problem with multi-phase Nano fluid in a partially divided cavity L×L are illustrated in Fig. 1.

Hydrodynamic and temperature boundary conditions for incompressible flow in cavity, respectively are as follows:

$$\begin{cases} u = 0 \\ v = 0 \end{cases} \quad at \begin{cases} x = 0 \\ x = L \end{cases}, \quad \begin{cases} y = 0 \\ y = L \end{cases} \tag{1}$$

$$\begin{aligned} &T = T_h \quad && at \quad x = 0, \quad 0 < y < L \\ &T = T_c \quad && at \quad x = L, \quad 0 < y < L \\ &\frac{\partial T}{\partial x} = 0 \quad && at \quad y = 0, \quad y = L, \quad 0 < x < L \end{aligned} \tag{2}$$

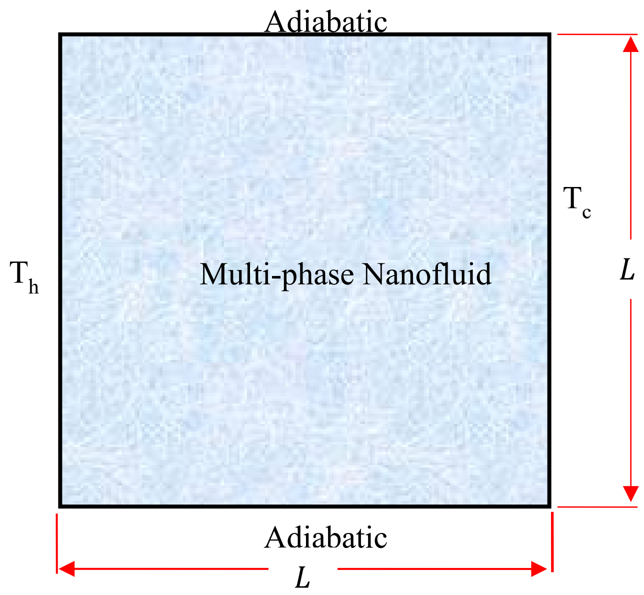

Fig. 1 - Schematic of Nano fluid solid – fluid cavity

In this investigation, we surveyed 4 shape of fins that arranged in three cases. Fig. 2 illustrated arrangement of rectangular, circle, vertical and horizontal ellipse fins in a partially divided cavity.

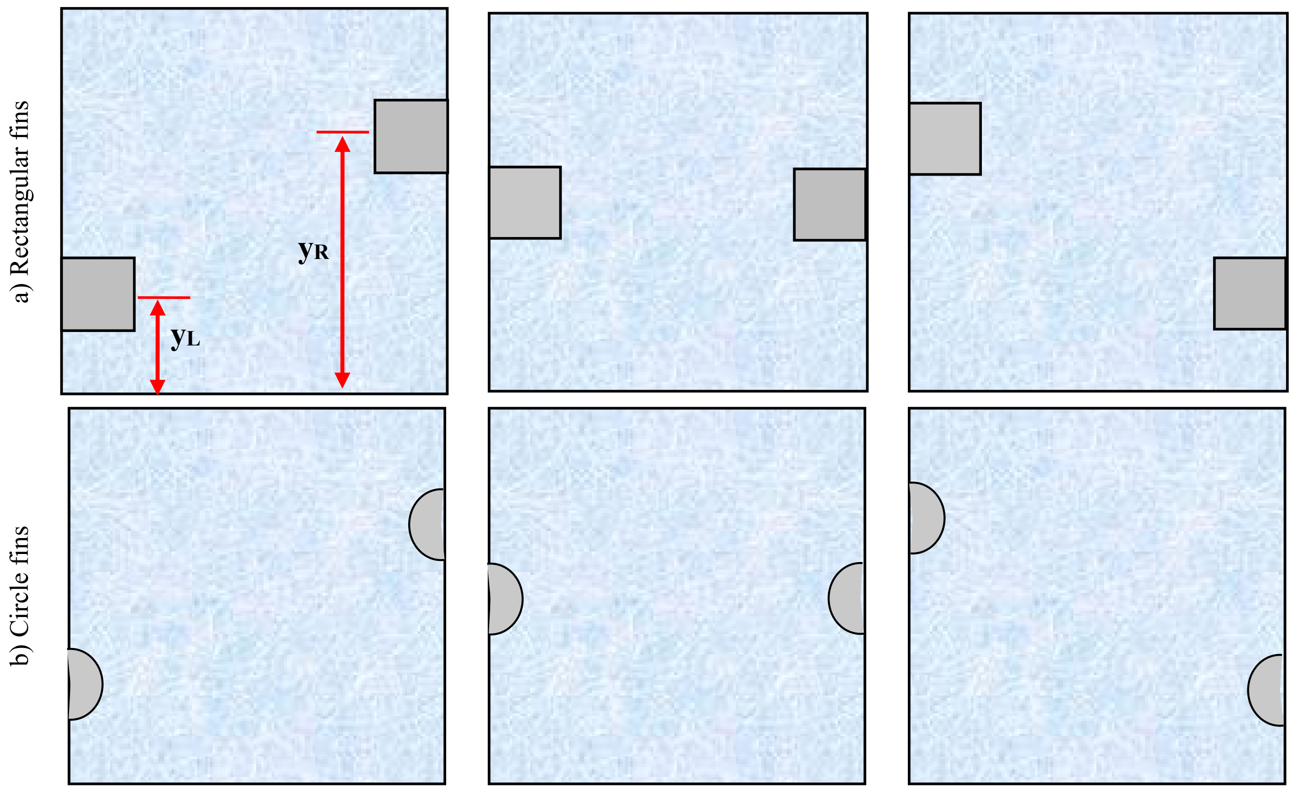

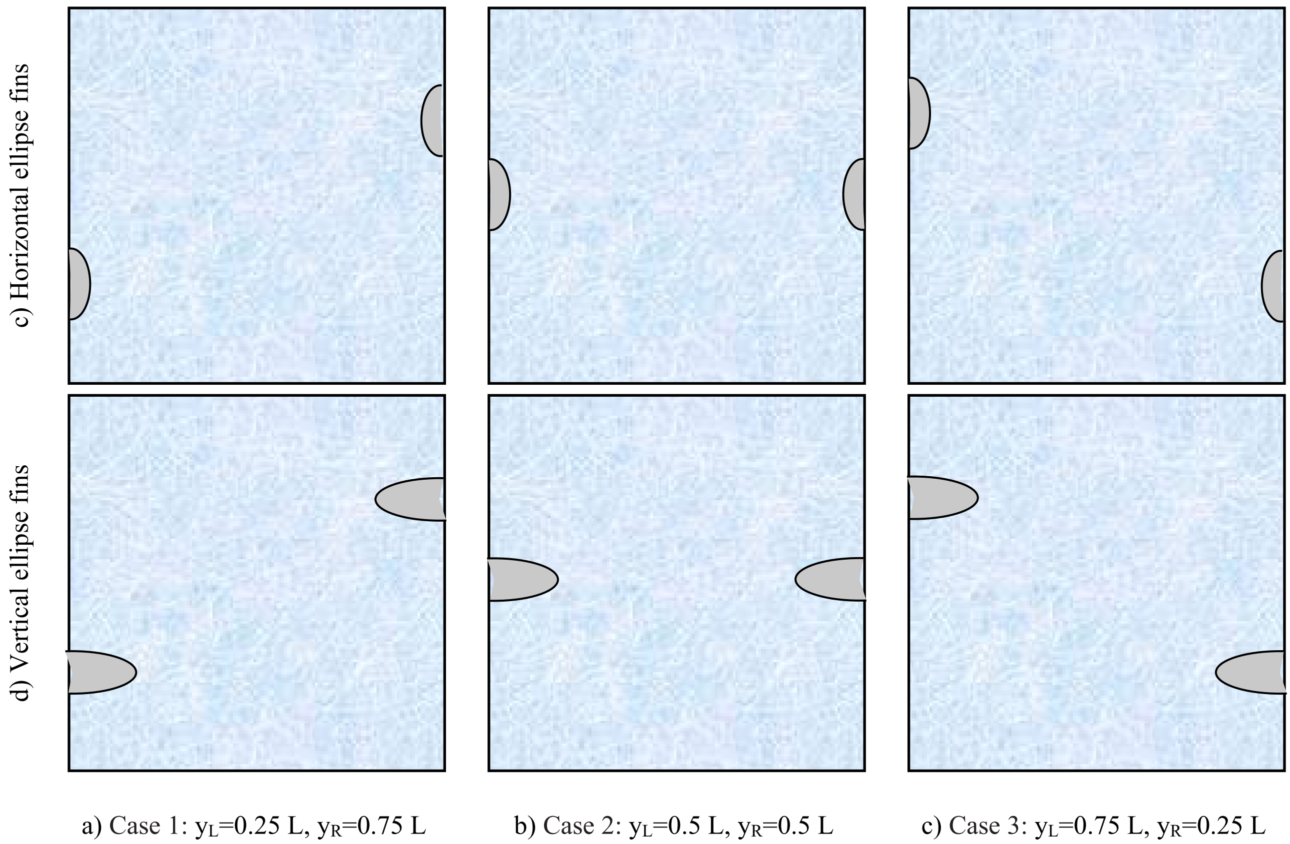

Fig. 2 - Schematics of different arrangement of fins in cavity

3. Simulation Methodology

3.1 Lattice Boltzmann Method

The present study examined two-dimensional flow by a 2D square lattice with nine velocities (D2Q9 model) and five temperature vectors (D2Q5 model) for modeling velocity of fluid and temperature fields, respectively. The velocity vectors c_0 ... c_8, of the D2Q9 model and temperature vectors c_0 ... c_4, of the D2Q5 model are shown in Fig. 3.

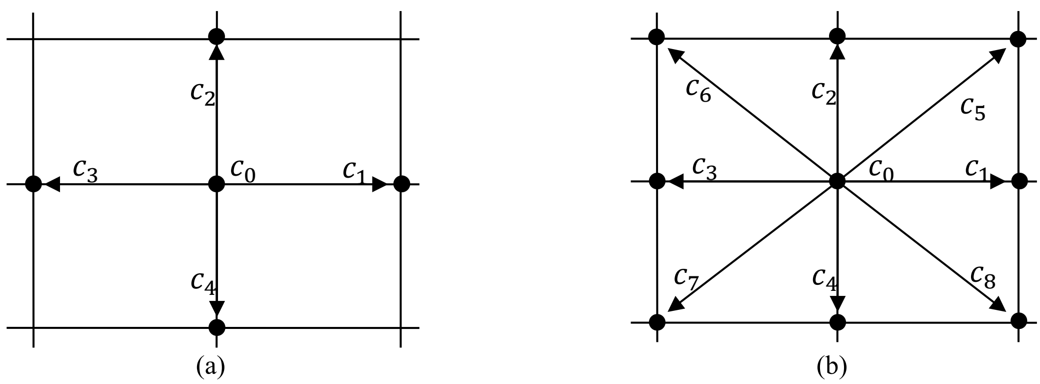

Fig. 3 - Two-dimensional vectors for (a) 5- temperature lattice; (b) 9-velocity lattice

The velocity and temperature vectors of the D2Q9 and D2Q5 models, respectively are represented in Table 1.

Table 1 - Velocity and temperature vectors of the D2Q9 and D2Q5 models

	K	0	1	2	3	4	5	6	7	8
D2Q9	c_k	(0,0)	$(1,0)c$	$(0,1)c$	$(-1,0)c$	$(0,-1)c$	$(1,1)c$	$(-1,1)c$	$(-1,-1)c$	$(1,-1)c$
D2Q5		(0,0)	$(1,0)c$	$(-1,0)c$	$(0,1)c$	$(0,-1)c$				

Where $c = \Delta x/\Delta t$ and k is the Lattice velocity direction. The two-phase Boltzmann's equation for a Nano fluid can be expressed as follows [20]:

$$f_i^\sigma(\mathrm{x} + \mathrm{e}_i\Delta t, t{+}\Delta t) - f_i^\sigma(\mathrm{x}, t) = -\frac{1}{\tau^\sigma}\left(f_i^\sigma(\mathrm{x}, t) - f_i^{\sigma,eq}(\mathrm{x}, t)\right) + \left(\frac{2\tau^\sigma - 1}{2\tau^\sigma}\right)\left(\frac{F_i^\sigma \cdot \mathrm{e}_i\Delta t}{B_i c^2}\right) + \Delta t F_i \tag{3}$$

Where $\sigma = 1, 2$ represent the base fluid and the nano-particle components of the nanofluid and τ_f^σ is the relaxation time of component σ, respectively. The equilibrium density distribution functions of the σth component, $f_i^{\sigma,eq}$ for the current 2D application, based on D2Q9 model, are expressed as:

$$f_i^{\sigma,eq}(x,t) = \omega_i\rho^\sigma\left[1 + \frac{3e_i \cdot u^{\sigma,eq}}{c^2} + \frac{9(e_i \cdot u^{\sigma,eq})^2}{2c^4} - \frac{3(u^{\sigma,eq})^2}{2c^2}\right] \tag{4}$$

The weight of velocity factors of the D2Q9 model are represented in Table 2.

Table 2 - Velocity vectors of the D2Q9 model

i	0	1	2	3	4	5	6	7	8
ω_i	$\frac{4}{9}$	$\frac{1}{9}$	$\frac{1}{9}$	$\frac{1}{9}$	$\frac{1}{9}$	$\frac{1}{36}$	$\frac{1}{36}$	$\frac{1}{36}$	$\frac{1}{36}$

The macroscopic density, kinematic viscosity and velocity of the σth component are given by $\rho^\sigma(\mathrm{x},t) = \sum_i f_i^\sigma(\mathrm{x},t)$, $\nu^\sigma = \frac{2\tau_f^\sigma - 1}{6}c^2\Delta t$ and $u^\sigma = \sum_i f_i^\sigma(x,t)e_i$ respectively. so, the equilibrium velocities $\mathrm{u}^{\sigma,eq}$ is given as:

$$u^{\sigma,eq} = \frac{1}{\rho^\sigma}\sum_i f_i^\sigma e_i + \frac{F^\sigma\tau_f^\sigma\Delta t}{\rho^\sigma} \tag{5}$$

The energy equation for Nano fluid, based on D2Q9 model represented as:

$$g_i^\sigma(x + e_i\Delta t, t + \Delta t) - g_i^\sigma(x,t) = \frac{1}{\tau_\theta^\sigma}\left[g_i^{\sigma,eq}(x,t) - g_i^\sigma(x,t)\right] \tag{6}$$

The equilibrium energy based on D2Q9 model represented as:

$$g_i^{\sigma,eq} = \omega_i T^\sigma\left[1 + \frac{e_i \cdot u^{\sigma,eq}}{c^2} + \frac{9(e_i \cdot u^{\sigma,eq})^2}{2c^4} - \frac{3(u^{\sigma,eq})^2}{2c^2}\right], \tag{7}$$

The weight of temperature factors of the D2Q5 model are represented in Table 3.

Table 3 - Velocity vectors of the D2Q5 model

i	0	1	2	3	4
ω_i	$\frac{2}{6}$	$\frac{1}{6}$	$\frac{1}{6}$	$\frac{1}{6}$	$\frac{1}{6}$

Where g_i^σ is the ith energy distribution function and τ_θ^σ is the thermal relaxation time and $T^\sigma = \sum_i g_i^\sigma$ is the temperature of the component σ. The corresponding thermal diffusivity is calculated as $\alpha^\sigma = \frac{2\tau_\theta^\sigma - 1}{6} c^2 \Delta t$. The buoyancy term is represented as:

$$F_H = \rho g \beta \Delta T \tag{8}$$

Where β is the thermal expansion coefficient and ΔT is the temperature difference. Thermophoresis force is [19]:

$$F_T = 3\pi\mu d_p \left(2A \frac{k}{2k + k_p} \frac{\mu}{\rho T}\right) \nabla T \tag{9}$$

Where A is the coefficient and (k, μ, ρ) and (k_p) are thermophysical properties of Nano fluid and particles, respectively. The drag force is obtained from Stokes law for small particles as follows [19]:

$$F_D = 3\pi\mu d_p (V - V_P) \tag{10}$$

Brownian motion is the random motion and the Brownian force represented as [19]:

$$F_B = C \frac{KT}{R} \tag{11}$$

Where C is a coefficient, K is the Boltzmann constant. In this survey, we used Al_2O_3 nanoparticles. So, Thermo-physical properties of Al_2O_3 nanoparticles are represented in Table 4.

Table 4 - Thermo-physical properties of water and Al_2O_3 nanoparticles

Material	ρ (kg/m^3)	C_P (J/kgK)	k (W/mK)	$\beta\times10^5$ (k^{-1})
Pure water	997.10	4179	0.61	21
Alumina (Al_2O_3)	3970	765	40	0.85

3.2 Parameters Specification

As an assessment way of natural convection problems, Nusselt number (Nu) is defined here by the temperature gradient as walls maintained at a constant temperature.

$$Nu_y = -\frac{H}{\Delta T}\left(\frac{\partial T}{\partial y}\right)_{wall} \tag{12}$$

$$Nu_m = \frac{1}{H}\int_0^H Nu_y dy \tag{13}$$

3.3 Validation for LBM

Figs. 4 and table 5 represented comparison of the temperature and velocity profiles. According to Figs. 4 the present simulation had acceptable accuracy and good agreement with M. Eslamian [21] in Ra=10^4 and Ra=10^6.

Table 5 - Comparison of the results with previous work on the symmetry plane of x=0.5

Ra	10^3	10^4	10^5	10^6	10^7	10^8
Grid used	80×80	80×80	80×80	80×80	80×80	100×100
Nu_m in present study	1.113	2.231	4.520	8.845	16.499	29.590
Nu_m in Ref. [46]	1.108	2.252	4.596	8.822	16.424	29.094

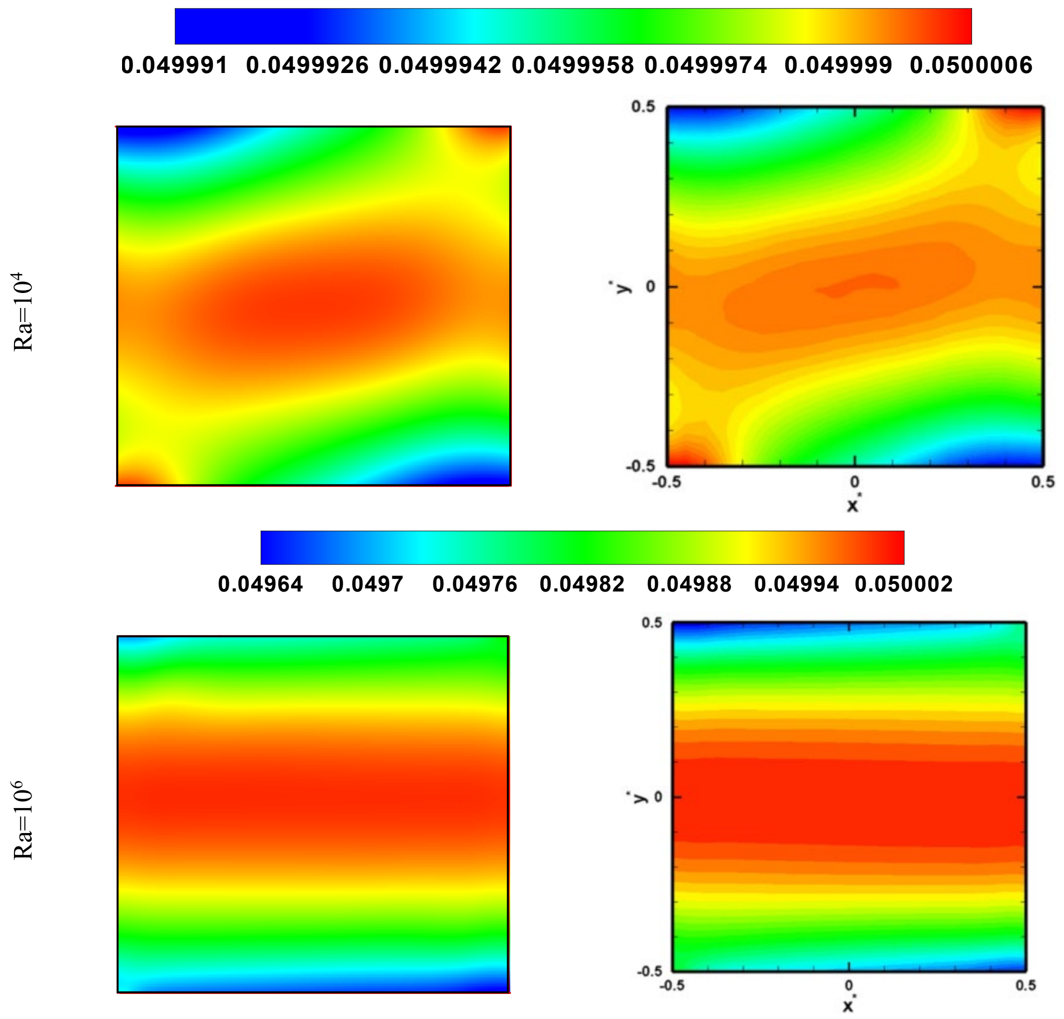

(a) (b)

Fig. 4 - Nanoparticle volume fraction distribution at Ra=10^6 in (a) present study; (b) Ref. [21]

4. Results and Discussion

Fig. 5 illustrated in cavity arranged with rectangular, circle, vertical and horizontal Ellipse fins, temperature fields in case 2: y_L=0.5 L, y_R=0.5 L are transferred more and faster than Case 3: y_L=0.75 L, y_R=0.25 L and Case 1: y_L=0.25 L, y_R=0.75 L, respectively. Also, temperature fields in cavity arranged with rectangular fins are transferred more and faster than cavity arranged with circle, vertical and horizontal Ellipse fins. Moreover, temperature fields in cavity arranged with vertical Ellipse fins are close to cavity with circle fins.

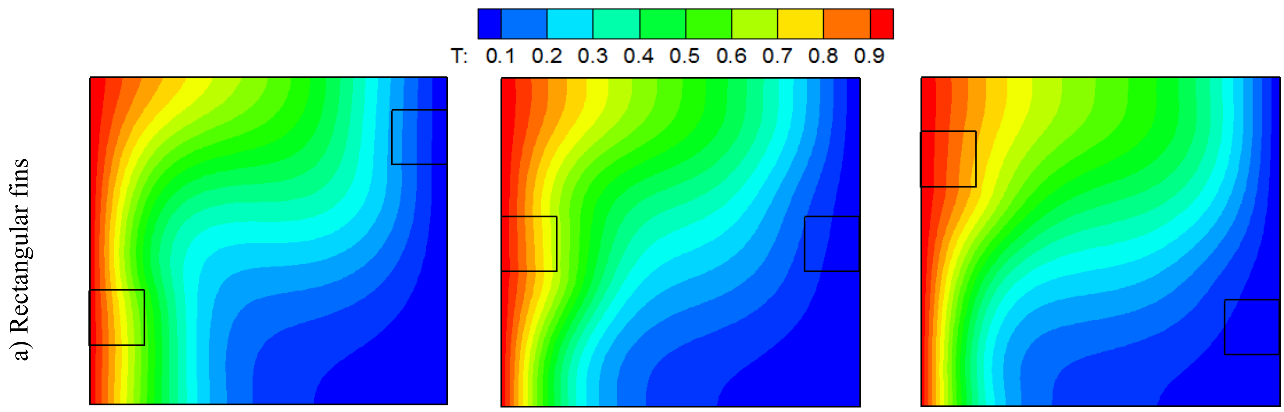

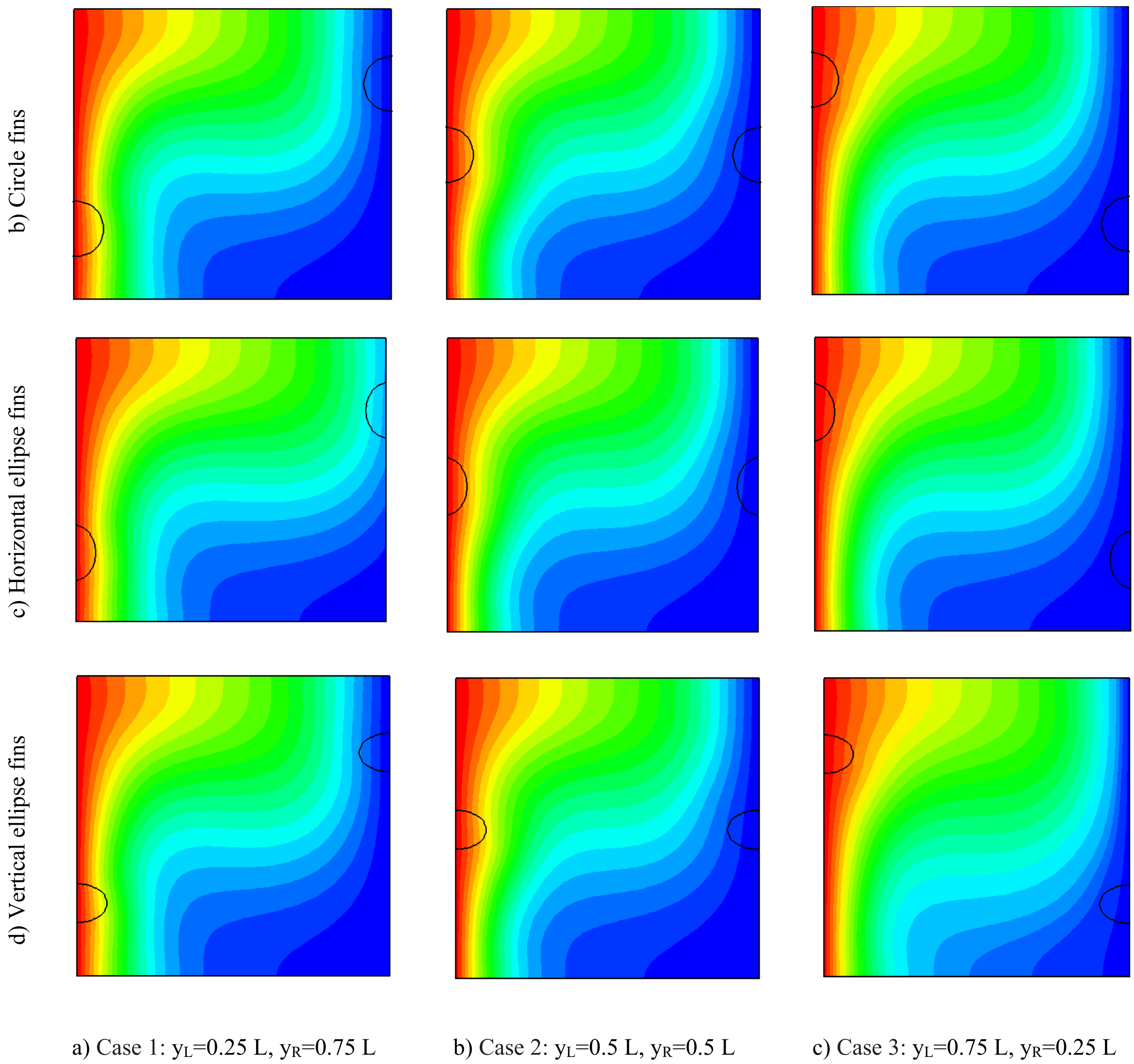

Fig. 5 - Comparison between temperature field in cavity with arrangement of different fins

In Fig. 6, temperature field on the middle surface of cavity $(y/L = 0.5)$ arranged with rectangular, circle, vertical and horizontal Ellipse fins are illustrated. All of cavities arranged with fins, in $0 < x < 0.5$, temperature fields on the middle surface of cavity in case 2: y_L=0.5 L, y_R=0.5 L are transferred more and faster than case 3: y_L=0.75 L, y_R=0.25 L and case 1: y_L=0.25 L, y_R=0.75 L, respectively. Also, in $0.5 < x < 1$, temperature fields on the middle surface of cavity are vice versa but these variations of temperature fields are less than position $0 < x < 0.5$. So, totally in $0 < x < 1$, variations of temperature fields are agreed with observations in Fig. 5.

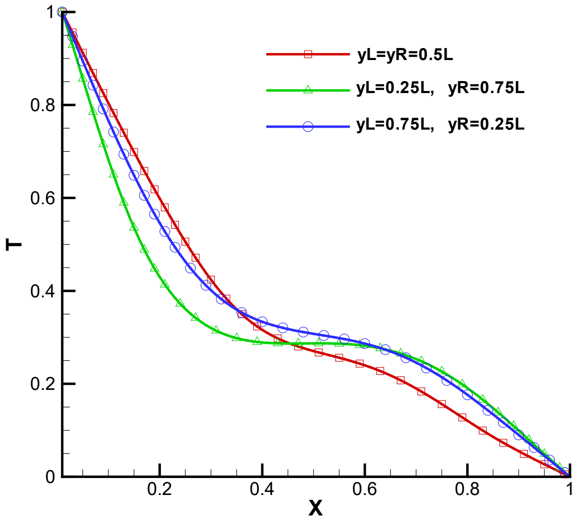

a) Rectangular fins

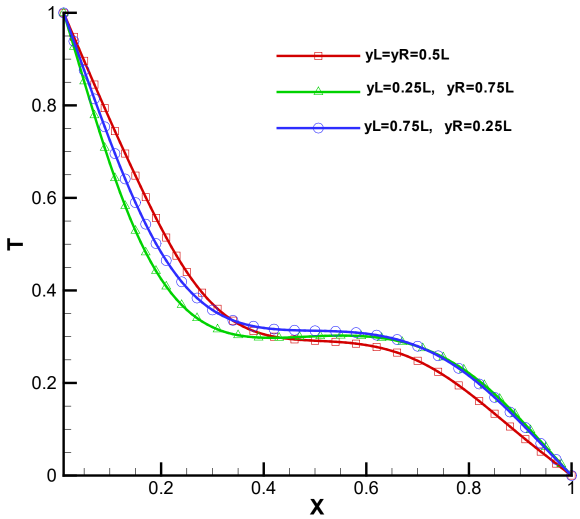

b) Circle fins

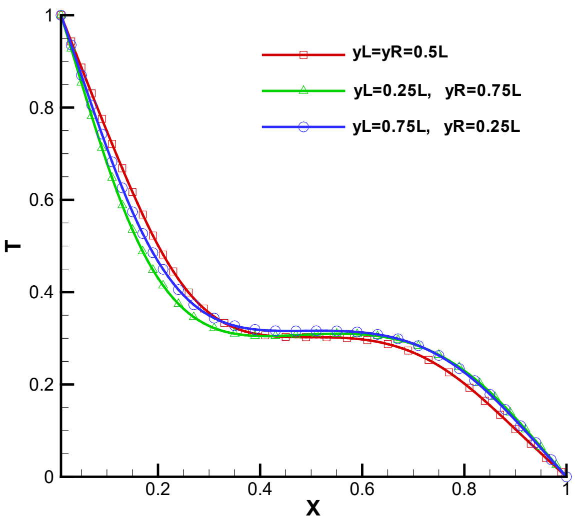

c) Horizontal ellipse fins

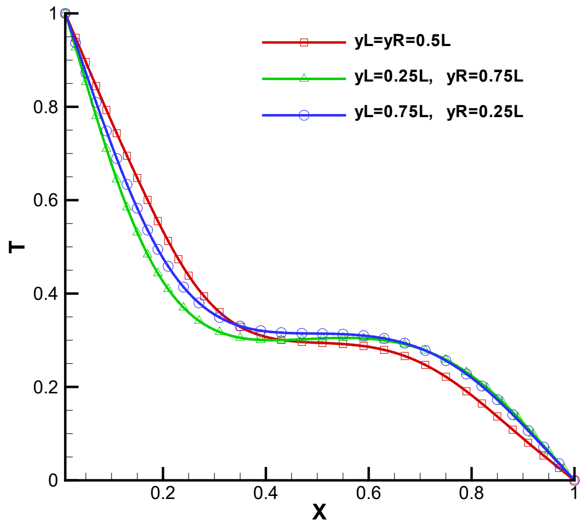

d) Vertical ellipse fins

Fig. 6 - Temperature field on the middle surface of cavity (y/L=0.5) with arrangement of different fins

Fig. 7 presented in all of cavities arranged with fins, velocity fields in case 2: y_L=0.5 L, y_R=0.5 L are transferred more and faster than other cases. Because Vortex flow in case 2 are less than other cases. Also, velocity fields in cavity arranged with rectangular fins are transferred more and faster than cavity arranged with circle, vertical and horizontal Ellipse fins, respectively.

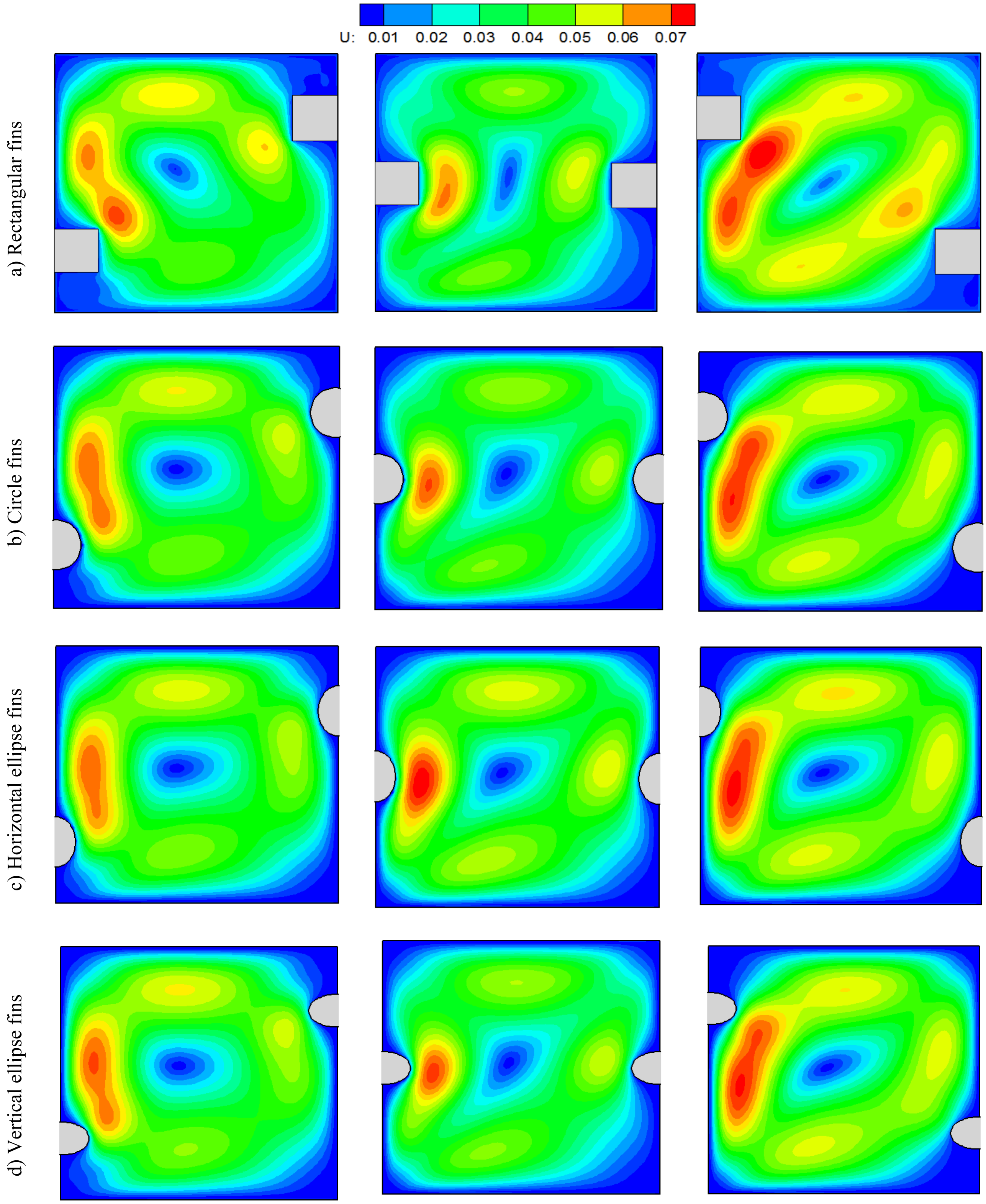

a) Case 1: y_L=0.25 L, y_R=0.75 L   b) Case 2: y_L=0.5 L, y_R=0.5 L   c) Case 3: y_L=0.75 L, y_R=0.25 L

Fig. 7 - Comparison between velocity field in cavity with arrangement of different fins

In Fig. 8, velocity field on the middle surface $(y/L = 0.5)$ of cavities arranged with all of fins are presented. According to observations, velocity fields on the middle surface of cavity in case 2: yL=0.5 L, yR=0.5 L are transferred more and faster than case 3: yL=0.75 L, yR=0.25 L and case 1: yL=0.25 L, yR=0.75 L, respectively. Also, in $0 < x <$

0.5, velocity fields on the middle surface of cavity in case: y_L=0.75 L, y_R=0.25 L are close to case 1: y_L=0.25 L, y_R=0.75 L in cavities arranged with all of fins. Moreover, velocity fields in cavity arranged with vertical Ellipse fins are almost similar to cavity with circle fins. So, consequently in $0 < x < 1$, variations of velocity fields are agreed with results in Fig. 7.

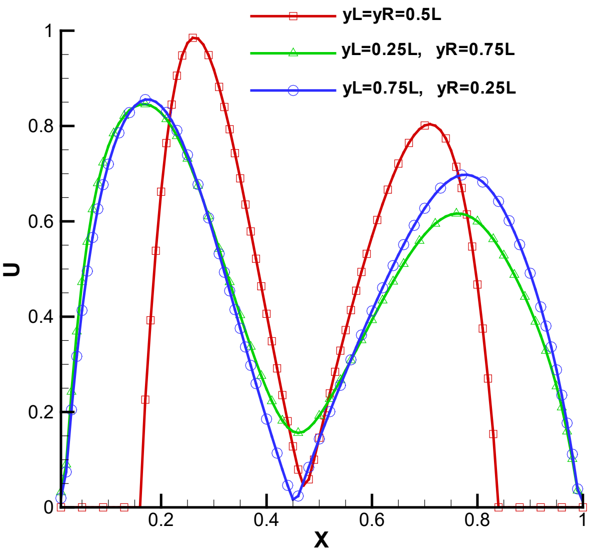

a) Rectangular fins

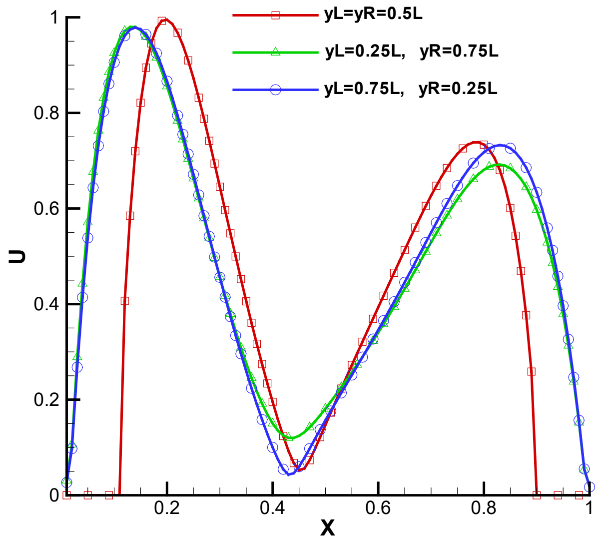

b) Circle fins

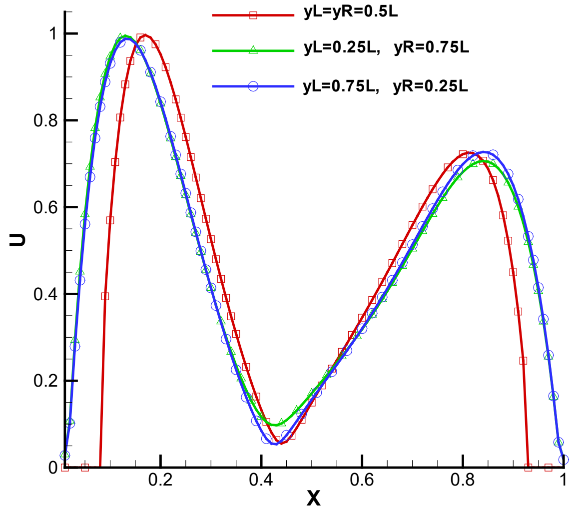

c) Horizontal ellipse fins

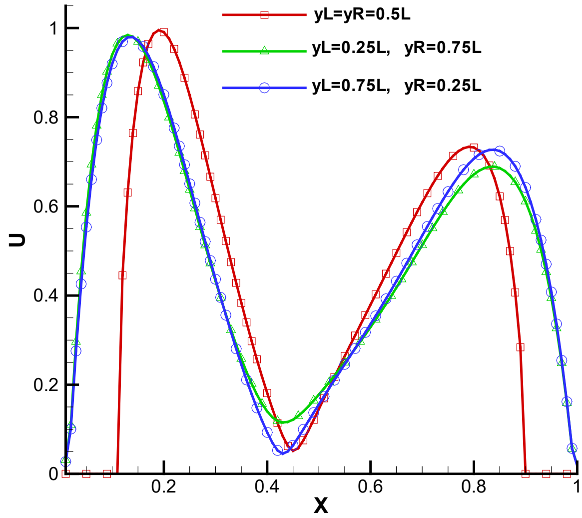

d) Vertical ellipse fins

Fig. 8 - Velocity field on the middle surface of cavity (y/L=0.5) with arrangement of different fins

In Fig. 9 illustrated in cavity arranged with rectangular, circle, vertical and horizontal Ellipse fins, Al_2O_3-water nanoparticles volume fraction in case 2: y_L=0.5 L, y_R=0.5 L was transferred to cold wall more than Case 1: y_L=0.25 L, y_R=0.75 L and Case 3: y_L=0.75 L, y_R=0.25 L, respectively. Also, nanoparticles volume fraction in cavity arranged with rectangular fins was transferred to cold wall more than cavities with other fins.

Fig.10 represented Nu number in cavities arranged with rectangular, circle, vertical and horizontal Ellipse fins. It is observed that in $0 < y < 0.5$, local Nusselt number in cavities arranged with all of fins, case 1: y_L=0.25 L, y_R=0.75 L was transferred to cold wall more than case 3: y_L=0.75 L, y_R=0.25 L and case 2: y_L=0.5 L, y_R=0.5 L, respectively. Also, in $0.5 < y < 1$, local Nusselt number in cavities arranged with all of fins, case 3: y_L=0.75 L, y_R=0.25 L was transferred to cold wall more than case 2: y_L=0.5 L, y_R=0.5 L and case 1: y_L=0.25 L, y_R=0.75 L, respectively.

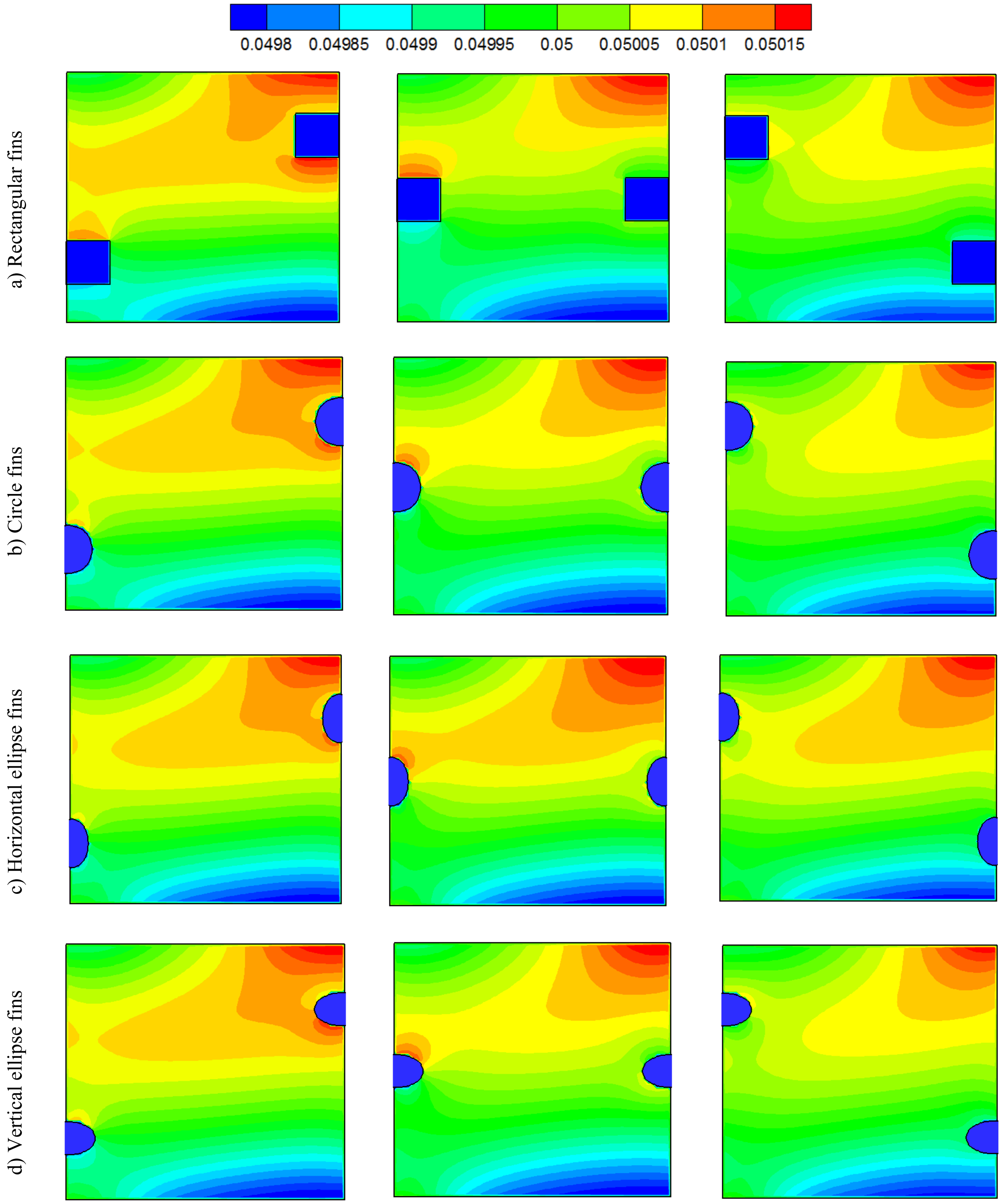

a) Case 1: y_L=0.25 L, y_R=0.75 L b) Case 2: y_L=0.5 L, y_R=0.5 L c) Case 3: y_L=0.75 L, y_R=0.25 L

Fig. 9 - Distribution of nanoparticle in cavity with arrangement of different fins

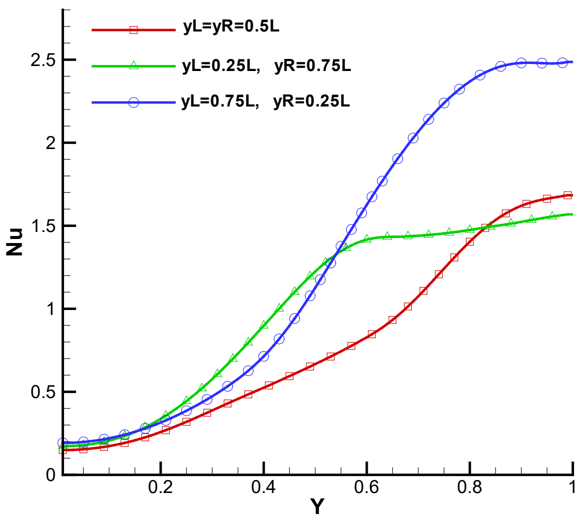

a) Rectangular fins

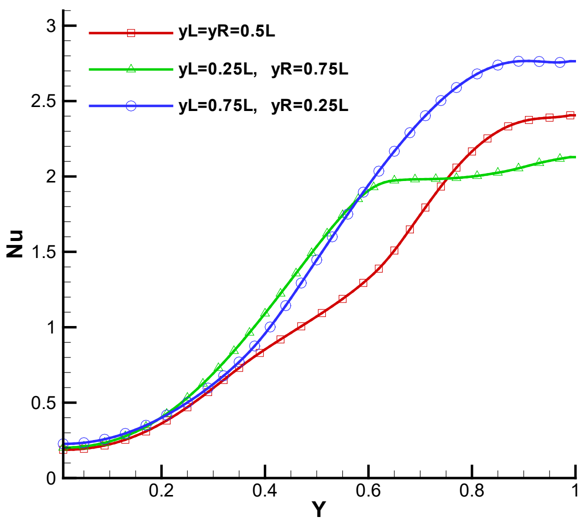

b) Circle fins

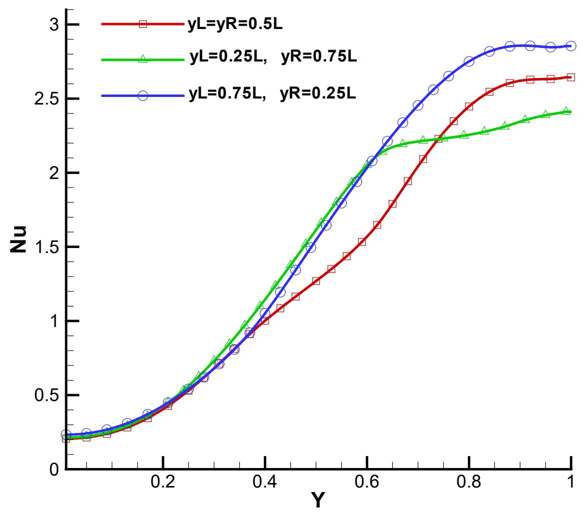

c) Horizontal ellipse fins

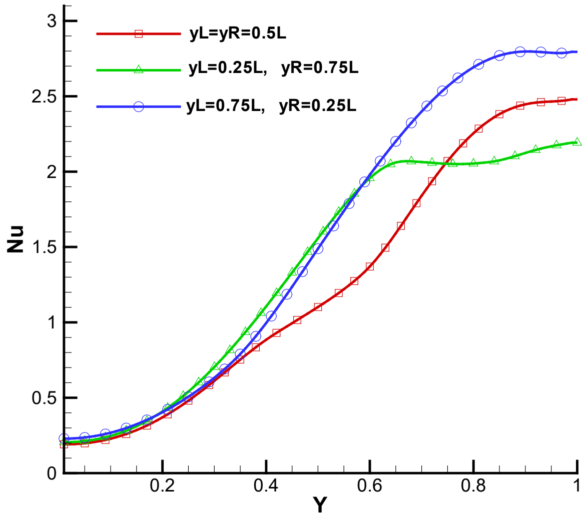

d) Vertical ellipse fins

Fig. 10 - Local Nu on the cold surface with arrangement of different fins

Table 6 is presented for Comparison Changes the mean Nu on the cold surface in cavities with the effect of fins and two-phase Al_2O_3-water Nano fluid. According to table, in all of cavities with different arrangement of fins, mean Nu on the cold surface in case 3: y_L=0.75 L, y_R=0.25 L was more than case 1: y_L=0.25 L, y_R=0.75 L and case 2: y_L=0.5 L, y_R=0.5 L. Also, cavities with horizontal ellipse fins had maximum Nusselt number more than vertical ellipse, circle and rectangular fins, respectively. Moreover, assuming case 2: y_L=0.5 L, y_R=0.5 L is base case, so with changing arrangement of fins for case 1: y_L=0.25 L, y_R=0.75 L, rate percentage of average Nusselt number for cavities arranged with rectangular, circle, vertical and horizontal Ellipse fins were %26, %8, %4 and %8, respectively. Furthermore, with changing arrangement of fins to case 3: y_L=0.75 L, y_R=0.25 L, these percentages were %62, %24, %14 and %22.

Table 6 - Mean Nu on the cold surface with arrangement of different fins

	Rectangular fins	**Circle fins**	**Horizontal ellipse fins**	**Vertical ellipse fins**
$y_L = y_R = 0.5L$	0.793	1.211	1.383	1.256
$y_L = 0.25L,\ \ y_R = 0.75L$	1.003	1.318	1.446	1.352
$y_L = 0.75L,\ \ y_R = 0.25L$	1.284	1.505	1.575	1.529

5. Conclusion

In this paper, a comprehensive numerical analysis fins shape and arrangement effects on Al_2O_3-water multi-phase nanofluid natural convection heat transfer in a partially divided cavity was investigated. The D2Q9 and D2Q5 LB method was used to solve the fluid flow and temperature field, respectively. Streamline, isotherm, nanoparticle volume fraction, Nusselt number, velocity and temperature fields were exhibited for arrangement rectangular, Circle, vertical and horizontal Ellipse fins. Finally, the main results summarized:

- Temperature, velocity and Al_2O_3-water nanoparticles volume fraction fields in case 2: yL=0.5 L, yR=0.5 L are transferred more and faster than Case 3: yL=0.75 L, yR=0.25 L and Case 1: yL=0.25 L, yR=0.75 L, respectively.
- Temperature fields in cavity arranged with rectangular fins are transferred more and faster than cavity arranged with circle, vertical and horizontal Ellipse fins.
- Assuming case 2: y_L=0.5 L, y_R=0.5 L is base case, so with changing arrangement of fins for case 1: y_L=0.25 L, y_R=0.75 L, rate percentage of average Nusselt number for cavities arranged with rectangular, circle, vertical and horizontal Ellipse fins were %26, %8, %4 and %8, respectively.
- with changing arrangement of fins to case 3: y_L=0.75 L, y_R=0.25 L, these percentages were %62, %24, %14 and %22.

Acknowledgements

The authors would like to thanks the Technical and Vocational University (TVU), Islamic Azad University, and Babol Noshirvani University of Technology for giving the opportunity to conduct this research.

References

[1] Samarbakhsh, S., and Alinejad, J., (2011). Experimental and Numerical Analysis of Eight Different Volutes with The Same Impeller in A Squirrel-Cage Fan. 2nd European conference of Control and Mechanical Engineering. 198-203.
[2] Alinejad, J., and Hoseinnejad, F., (2012). Aerodynamic Optimization in The Rotor of Centrifugal Fan Using Combined Laser Doppler Anemometry and CFD Modeling. World Applied Sciences Journal, 17, 10. 1316-1323.
[3] Alinejad, J., Montazerin, N., and Samarbakhsh, S., (2013). Accretion of The Efficiency of a Forward-Curved Centrifugal Fan by Modification of the Rotor Geometry: Computational and Experimental Study. International Journal of Fluid Mechanics Research, 40, 6, 469-481.
[4] Esfahani, J. A., and Alinejad, J., (2013). Lattice Boltzmann Simulation of Viscous-Fluid Flow and Conjugate Heat Transfer in A Rectangular Cavity with A Heated Moving Wall. Thermophysics and Aeromechanics, 20, 5, 613-620.
[5] Esfahani, J. A., and Alinejad, J., (2013). Entropy Generation of Conjugate Natural Convection in Enclosures: The Lattice Boltzmann Method. International Journal of Multiphase Flow, 27, 3, 498-505.
[6] Alinejad, J., and Esfahani, J. A., (2014). Lattice Boltzmann Simulation of Forced Convection Over an Electronic Board with Multiple Obstacles. Heat Transfer Research, 45, 3, 241-262.
[7] Alinejad, J., and Esfahani, J. A., (2016). Numerical Stabilization of Three-Dimensional Turbulent Natural Convection Around Isothermal Cylinder. Journal of Thermophysics and Heat Transfer, 30, 1, 94-102.
[8] Alinejad, J., and Esfahani J., A., (2016). Lattice Boltzmann Simulation of EGM and Solid Particle Trajectory Due to Conjugate Natural Convection. Aerospace Science and Technology, 4, 1, 36-43.
[9] Alinejad, J., and Fallah, K., (2016). Taguchi Optimization Approach for Three-Dimensional Nanofluid Natural Convection in a Transformable Enclosure. Journal of Thermophysics and Heat Transfer, 31, 1, 1-7.
[10] Alinejad, J., and Esfahani J., A., (2017). Taguchi Design of Three Dimensional Simulations for Optimization of Turbulent Mixed Convection in A Cavity. Meccanica, 52, 4-5, 925-938.
[11] Alinejad, J., and Esfahani J., A., (2016). Optimization of 3-D Natural Convection Around the Isothermal Cylinder Using Taguchi Method. Journal of Applied Mechanics and Technical Physics, 57, 1, 117-126.
[12] Fallah, K., Gerdroodbary, M., B., Ghaderi, A., and Alinejad, J., (2018). The Influence of Micro Air Jets On Mixing Augmentation of Fuel in Cavity Flameholder at Supersonic Flow. Aerospace Science and Technology, 76, 1, 187-193.
[13] Peiravi, M. M., Alinejad, J., Domairry Ganji, D., and Maddah, S., (2019). Numerical Study of Fins Arrangement and Nanofluids Effects On Three-Dimensional Natural Convection in The Cubical Enclosure. Transp Phenom Nano Micro Scales, 7, 2, 97-112.
[14] Peiravi, M. M., and Alinejad, J., (2019). Hybrid Conduction, Convection and Radiation Heat Transfer Simulation in A Channel with Rectangular Cylinder. Journal of Thermal Analysis and Calorimetry, 140. 2733-2747.
[15] Peiravi, M. M., and Alinejad, J., (2021). Nano Particles Distribution Characteristics in Multi-Phase Heat Transfer Between 3D Cubical Enclosures Mounted Obstacles. Alexandria Engineering Journal, 60, 6, 5025-5038.
[16] Alinejad, J., and Peiravi, M. M., (2020). Numerical Analysis of Secondary Droplets Characteristics Due to Drop Impacting On 3D Cylinders Considering Dynamic Contact Angle. Meccanica, 55, 10, 1975–2002.

[17] Peiravi, M. M., Alinejad, J., Domairry Ganji, D., and Maddah, S., (2019). 3D Optimization of Baffle Arrangement in A Multi-Phase Nanofluid Natural Convection Based On Numerical Simulation. International Journal of Numerical Methods for Heat and Fluid Flow, 30. 2583-2605.

[18] Domairry Ganji, D., Peiravi, M. M., and Abbasi, M., (2015). Evaluation of The Heat Transfer Rate Increases in Retention Pools Nuclear Waste. International Journal of Nano Dimension. International Journal of Nano Dimension, 6, 4, 385-398.

[19] Mezrhab, A., Jami, M., Abid, C., Bouzidi, M., and Lallemand, P., (2006). Lattice Boltzmann Modeling of Natural Convection in an Inclined Square Enclosure with Partitions Attached to Its Cold Wall. International Journal of Heat and Fluid Flow, 27, 3, 456-465.

[20] Nourgaliev, R. R., Dinh, T. N., Theofanous, T. G., and Joseph, D., (2003). The Lattice Boltzmann Equation Method: Theoretical Interpretation, Numerics and Implications. International Journal of Multiphase Flow, 29, 1, 117-169.

[21] Ahmed, M, and Eslamian, M., (2014). Natural Convection in A Differentially-Heated Square Enclosure filled with A Nanofluid: Significance of The Thermophoresis Force and Slip/Drift Velocity. International Communications in Heat and Mass Transfer, 58, 4, 1–11.